Modeling of the Coal Gasification Processes in a Hybrid Plasma Torch

Igor B. Matveev and Serhiy I. Serbin

***Abstract*—The major advantages of the plasma treatment systems are cost effectiveness and technical efficiency. A new efficient electrodeless 1 MW hybrid plasma torch for waste destruction and coal gasification is proposed. This product will merge several solutions, as known inductive type plasma torch, innovative reverse vortex reactor and recently developed non-equilibrium plasma pilot and plasma chemical reactor. With the use of CFD-computational method preliminary 3D calculations of heat exchange in a 1 MW plasma generator operating with direct and reverse vortexes have been conducted at the air flow rate of 100 g/s. For investigated mode and designed parameters reduction of the total wall heat transfer for the reverse scheme is about 65 kW that corresponds to increasing of the plasma torch efficiency approximately on 6.5 %. This new hybrid plasma torch will operate as a multi-mode, high power plasma system with wide range of plasma feedstock gases and turn down ratio, convenient and simultaneous feeding of several additional reagents into the discharge zone.**

***Index Terms*—Coal, modeling, plasma, waste processing.**

I. Introduction

THE need for the ultimate waste destruction offered by plasma technology is evident from population growth in all nations, deterioration of water supplies, increased production of toxic wastes and infectious hospital wastes, and the diminishing amount of land that can be used for municipal solid waste dumps. Because of these increasing volumes of all types of wastes and the increased risk to human health associated with such growth, it is prudent to use a technology that offers the destruction of wastes and does not generate new toxic wastes. The major advantages of plasma treatment systems are cost effectiveness and technical efficiency. Upon acceptance of the waste stream, the plasma system destroys organics creating harmless elemental gases and particulate and at the same time reduces inorganic oxides to a glass-like byproduct. As it destroys the wastes, the plasma system can create salable by-products, which offset operating costs and have value to society, e.g., hot water for district heating, steam for industrial and hospital use, fuel gas for heating, and aggregate for a variety of uses.

Coal gasification offers one of the most versatile and clean ways to convert coal into electricity, hydrogen, and other energy forms. Plasma steam coal gasification looks like the best solution for portable and small to media-scale coal processing facilities.

One of the major obstacles on the way of above plasma technologies implementation is limited lifetime of existing plasma torches, which does not exceed 100-150 hours for 300-500 kW DC and AC devices. That's why development and production of innovative high power, universal, atmospheric pressure plasma torches with dramatically improved performance and extended durability is a significant challenge.

Applied Plasma Technologies (APT) develops high energy efficient, robust, durable, universal, electrodeless 1 MW hybrid plasma reformer mainly for waste destruction and coal gasification. This product will merge several solutions, as known inductive type plasma torch, innovative reverse vortex reactor and recently developed by APT non-equilibrium plasma pilot and plasma chemical reactor [1-5]. The APT's solution will improve existing and operating in vacuum 1 MW plasma torch by: (1) utilizing and further development of known reverse vortex flow and implement this technology for gas turbine combustors and some plasma generators; (2) applying novel non-equilibrium plasma pilot and plasma chemical reactor for the main plasma torch excitation, reagents feeding and their initial activation; (3) converting a vacuum operating unit into an atmospheric pressure device. All this will result in development of the generic high power atmospheric pressure plasma torch with:

a) simple, electrodeless design with almost endless lifetime for operation on a wide variety of plasma feedstock gases as air, N_2, CO_2, Ar, and different blends in a wide range of pressure and flow rates;

b) reduced heat losses due to the "cold wall" effect of the reverse vortex flow, which allows higher performance, cheaper materials, lower maintenance costs;

c) opportunity to work on different modes as a plasma torch, plasma chemical reactor, plasma assisted fuel converter, multi-fuel plasma assisted combustor, etc.

General view of a triple vortex plasma reformer is shown in Fig. 1. This is a hybrid system because consists of an inductive RF heater with power up to 1 MW and a number of bottom placed high voltage DC plasma torches. These torches serve for initial media ionization inside the reactor, fuel and additional reagents feeding. The system will operate as a multi-mode, multi-purpose reactor in a wide range of plasma feedstock gases and turn down ratios, convenient and

Manuscript received February 15, 2007.

I. Matveev is with the Applied Plasma Technology, McLean, VA 22101 USA (phone: 703-560-9569; fax: 703-849-8417; e-mail: i.matveev@att.net).

S. Serbin is with the National University of Shipbuilding, 9 Geroev Stalingrada Ave., Mykolayiv, 54025, Ukraine (phone: +380-512-398-135; fax: +380-512-424-652; e-mail: serhiy@serbin.mk.ua).

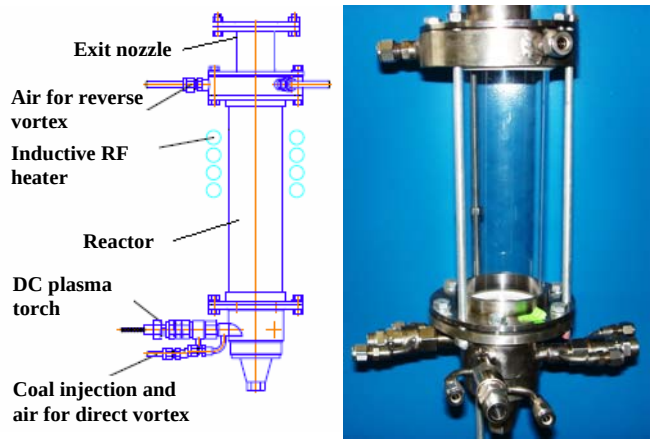

Fig. 1. Diagram and picture of the triple vortex plasma reformer.

simultaneous feeding of several additional reagents, for example coal and air, into the discharge zone. Reverse and direct vortex air streams are injected separately through the tangential channels of vortex generators located near the exit nozzle and the bottom part accordingly. General view of the reverse vortex hybrid plasma torch without coil according to recent patent application [1] is shown in the picture above.

Flow schematic inside the reactor [1] is shown in Fig.2. Coal for processing could be injected either with air for direct vortex generation or by means of a coal feeder. In the direct vortex (DV) mode the swirl generator is placed upstream the RF discharge zone and the DC plasma torch plums create an additional swirling effect. In such systems with intensive flow

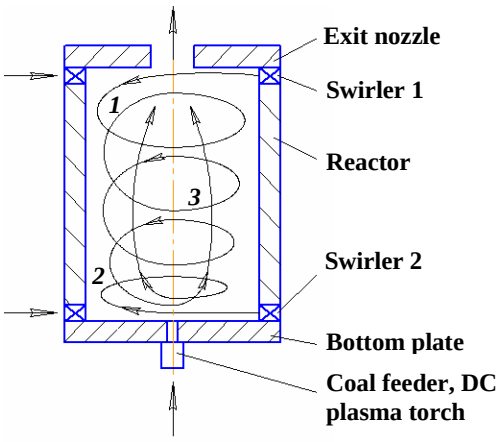

Fig. 2. Flow schematic inside the reactor.

rotation the cross sectional pressure distribution with minimum values on the axis near the vortex generator is spatially deeper than downstream. As a result, a central reverse flow forms and transfers energy from the RF plasma area to the recirculation zone created by DC torches and the bottom swirlers. The hot, reverse flow mixes with incoming cold direct vortex flow. After mixing, the direct vortex *2* of hot reagents moves along the walls of the hybrid plasma torch loosing significant part of its thermal energy due to intensive heat transfer through the walls. It's obvious that the plasma torch with direct vortex flow needs appropriate walls cooling.

The main idea of the reverse-vortex (RV) stabilization in a hybrid plasma torch is to direct the main stream of cold swirling plasma feedstock gas named the first (reverse) vortex *1* along the walls from the inlet point near the exit nozzle to the torch bottom, mix with the second (direct) vortex *2* of feeding reagents and create the third vortex *3* of reacting species inside the first one. Cold reverse plasma feedstock gas flows along the wall to the closed bottom end, and turbulent micro-volumes of this cold gas, which lost their kinetic energy near the wall, migrate radially towards the centre. As a result, cold air comes into the hot plasma zone from all sides, except the outlet side, and no significant recirculation zone is formed.

It was found that, in case of a microwave plasma generator with total power of 3.5 kW simple system modification from DV to RV resulted in a significant increase in thermal efficiency: in an experimental RV plasma generator the heat loss was 4-7 %, and in an industrial DV plasma generator of the same geometry the heat loss level was 26-42 %, depending on gas consumption [5]. Such promising results encourage applying RV for high temperature inductive reformation system.

In contrast to scheme suggested by Dr. Gutsol at al [6, 7] the proposed triple vortex plasma reformer has the third vortex which forms higher concentration of coal and oxidizer in a mixing region adjacent to the coal inlet and serves as a mean to create high level of turbulence in the mixing area to improve the reactor's performance. Besides, possibilities for the plasma reformer regulation are significantly increased as a consequence of opportunity to adjust location of the direct and reverse vortexes contact zone by the flow rates changing.

Inductively coupled plasma (ICP) torches (or radio frequency (RF) plasma generators) are widely applied, mainly for high temperature treatment and plasma spray deposition of materials, densification and spheroidization of powders, chemical synthesis of nano-particles, waste treatment. Detailed experimental diagnostics of such kind of devices is very hard to perform, owing to the high temperatures involved and to the difficulty of reaching the internal zones without perturbing the discharge. As an alternative, mathematical modeling represents a valid and powerful tool to predict the characteristics of this kind of a system. A number of publications [6-13] have been devoted to the numerical simulation of the high temperature plasma flow within the RF plasma generator discharge chamber. In the most part of these papers the problem is considered in the local thermo-chemical equilibrium. Only recently the non-equilibrium plasma calculations have been arisen. In order to obtain more realistic description of an ICP torch, a fully 3D model [8–10] has been developed. The model has been implemented in the framework of the computational fluid dynamics (CFD) commercial software FLUENT®, using a grid extending also outside the plasma region for the treatment of the electromagnetic field. But papers coupled with numerical CFD simulation of coal gasification processes in inductive plasma reformers are practically missed.

The current paper objectives are: (1) theoretical CFD investigations of the coal gasification processes inside the plasma reformer and (2) analysis of the inductive type 1 MW plasma torch thermal efficiency improved by application of the reverse vortex flow.

II. Modeling of the Coal Gasification Processes in Inductive Type Plasma Torch

A. Modeling of Basic Fluid Flow in Inductive Type Plasma Torch

For modeling of basic flow processes inside the inductive atmospheric pressure plasma torch a generalized method has been used, based on numerical solution of the combined conservation and transport equations for turbulent system [12, 14-19]. This method provides a procedure of the numerical integration of the 3D-differential equations that describe viscous gas flows: the equations for conservation of mass, momentum, and energy.

The equation for conservation of mass can be written as follows:

$$\frac{\partial \rho}{\partial t} + \nabla \cdot (\rho \vec{v}) = S_m .$$

This equation is the general form of the mass conservation equation and is valid for incompressible as well as compressible flows. The source S_m is the mass added to the continuous phase from the dispersed second phase and any user-defined sources.

The equation for conservation of momentum:

$$\frac{\partial}{\partial t}(\rho \vec{v}) + \nabla \cdot (\rho \vec{v} \vec{v}) = -\nabla p + \nabla \cdot (\tau_{st}) + \rho \vec{g} + \vec{F} + \vec{J} \times \vec{B}$$

where p is the static pressure, τ_{st} is the stress tensor, $\rho \vec{g}$ and $\vec{F}$ are the gravitational body force and external body forces, respectively, $\vec{F}$ contains other model-dependent source terms such as user-defined sources, $\vec{J}$ is the current density vector, $\vec{B}$ is the magnetic induction.

The energy equation:

$$\frac{\partial}{\partial t}(\rho E) + \nabla \cdot (\vec{v}(\rho E + p)) = \nabla \cdot (k_{eff} \nabla T - \sum_j \vec{J}_j + (\vec{\tau}_{eff} \cdot \vec{v})) + S_h + \vec{J} \times \vec{E}$$

where k_{eff} is the effective conductivity ($k + k_t$, where k_t is the turbulent thermal conductivity, defined according to the turbulence model being used), $\vec{J}_j$ is the diffusion flux of species j, and $\vec{E}$ is the electric field strength vector. The first three terms on the right-hand side of this equation represent energy transfer due to conduction, species diffusion, and viscous dissipation, respectively. S_h includes the heat of chemical reaction, and any other volumetric heat sources.

The electromagnetic field generated by the current in the coil, $\vec{J}_c$ and by the induced currents in the plasma can be described with the help of the Maxwell's equations in the vector potential form [12]:

$$\nabla^2 \vec{H} - i\omega\mu_0\sigma\vec{H} + \mu_0 \vec{J}_c = 0$$

where μ_0 is the magnetic permeability of the free space, σ is the plasma electrical conductivity, $\omega = 2\pi f$, f is the frequency of the electromagnetic field.

The electric field $\vec{E}$ and the magnetic field $\vec{B}$ vectors can be obtained from the vector potential $\vec{H}$ with the following expressions [12]:

$$\vec{E} = -i\omega\vec{H}\ , \quad \vec{B} = \nabla \times \vec{H}\ ,$$

and from the simplified Ohm's law $\vec{J} = \sigma\vec{E}$.

Application of the Maxwell's equations with commercial software fluid dynamic modules allows carry out the 3D investigation of different coil shapes, torch geometries and operating conditions [12]. But this technique considerably complicates the computing scheme, rises instability of numerical solution. That is not always justified when it is necessary to conduct the preliminary efficiency estimations of different schemes of working process organization in the plasma reformer. Therefore with the purpose of more detailed modeling of the coal gasification processes inside the inductive plasma torch the simplified (preliminary) approach is used, according to which the volume of heat release zone (Fig. 3) is assumed to be known from experimental data. In this case the sources of energy in the energy equation include the source due to chemical reaction, and additional volumetric heat sources (when the Maxwell's equations are not solved):

$$S_h = -\sum_j h_j^0 R_j / M_j + E_V$$

where h_j^0 is the enthalpy of formation of species j, R_j is the volumetric rate of creation of species j, E_V is the volumetric energy source

$$E_V = P_p / V$$

where P_p is the plasma torch power, V is the volume of heat release zone (from experiment [20, 21]).

Additional transport equations are also solved when the flow is turbulent. For aerodynamic prediction the RNG-based k-ε -turbulence model was used. This model is derived from the instantaneous Navier-Stokes equations, using a mathematical technique called "renormalization group" (RNG) methods [22]. The main difference between the RNG and standard k-ε -models lies in the additional term in the ε equation.

The turbulence kinetic energy, k, and its rate of dissipation, ε, are obtained from the following transport equations:

$$\frac{\partial}{\partial t}(\rho k)+\frac{\partial}{\partial x_i}(\rho k u_i)$$
$$=\frac{\partial}{\partial x_j}(\alpha_k \mu_{eff}\frac{\partial k}{\partial x_j})+G_k+G_b-\rho\varepsilon-Y_M+S_k,$$
$$\frac{\partial}{\partial t}(\rho\varepsilon)+\frac{\partial}{\partial x_i}(\rho\varepsilon u_i)$$
$$=\frac{\partial}{\partial x_j}(\alpha_\varepsilon \mu_{eff}\frac{\partial \varepsilon}{\partial x_j})+C_{1\varepsilon}\frac{\varepsilon}{k}(G_k+C_{3\varepsilon}G_b)-C_{2\varepsilon}\rho\frac{\varepsilon^2}{k}-R_\varepsilon+S_\varepsilon,$$
$$\mu_{t0}=C_\mu\rho k^2/\varepsilon,\quad \mu_t=\mu_{t0}f(\alpha_s,\Omega,\frac{k}{\varepsilon}),$$
$$R_\varepsilon=\frac{C_\mu\rho\eta^3(1-\eta/\eta_0)}{1+\beta\eta^3}\frac{\varepsilon^2}{k},\ \eta=Sk/\varepsilon.$$

In these equations, μ_{eff} is the effective viscosity, G_k represents generation of a turbulence kinetic energy due to the mean velocity gradients, G_b is the generation of turbulence kinetic energy due to buoyancy, Y_M represents the contribution of the fluctuating dilatation in compressible turbulence to the overall dissipation rate. The quantities α_k and α_ε are the inverse effective Prandtl numbers for *k* and ε, respectively, S_k and S_ε are user-defined source terms, $C_{1\varepsilon}$, $C_{2\varepsilon}$, $C_{3\varepsilon}$ are the constants of turbulence model, μ_{t0} is the value of turbulent viscosity calculated without the swirl modification, Ω is the characteristic swirl number, α_s is the swirl constant.

In the simulation the constants of the RNG $k-\varepsilon$ turbulence model have been used: $C_{1\varepsilon}=1.42$, $C_{2\varepsilon}=1.68$, $C_\mu=0.0845$, $\alpha_k=\alpha_\varepsilon=1.393$, $\eta_0=4.38$, $\beta=0.012$, $\alpha_s=0.07$ [16, 22].

In comparison with the standard *k*-ε -model, the smaller destruction of ε augments, reducing k and, eventually, the effective viscosity. As a result, in rapidly strained flows, the RNG model yields a lower turbulent viscosity than the standard *k*-ε -model. Thus, the RNG model is more responsive to the effects of rapid strain and streamline curvature than the standard *k*-ε -model, which explains the superior performance of the RNG model for certain classes of flows.

B. Coal Gasification Modeling

If chemical reactions take place it is necessary to solve conservation equations for chemical species and to predict the local mass fraction of each species through the solution of a convection-diffusion equation for the j-th species. This conservation equation takes the following form:

$$\frac{\partial}{\partial t}(\rho Y_j)+\nabla\cdot(\rho\vec{v}Y_j)=-\nabla\cdot\vec{J}_j+R_j+S_j$$

where Y_j, R_j are the mass fraction and net rate of production of species j by chemical reaction, S_j is the rate of creation by addition from the dispersed phase plus any another sources.

For coal gasification calculations in a hybrid plasma torch the FLUENT coupled discrete phase model (DPM) was used. Procedure predicts the trajectory of a discrete phase particle by integrating the force balance on the particle, which is written in a Lagrangian reference frame. This force balance equates the particle inertia with the forces acting on the particle, and can be written (for the x direction in Cartesian coordinates) as

$$\frac{du_p}{dt}=F_D(u-u_p)+\frac{g_x(\rho_p-\rho)}{\rho_p}+F_x$$

where F_x is an additional acceleration term, $F_D(u-u_p)$ is the drag force per unit particle mass and

$$F_D=\frac{18\mu}{\rho_p d_p^2}\frac{C_D\,\mathrm{Re}}{24}.$$

Here, u is the fluid phase velocity, u_p is the particle velocity, μ is the molecular viscosity of the fluid, ρ is the fluid density, ρ_p is the density of the particle, d_p is the particle diameter, Re is the relative Reynolds number.

The turbulent dispersion of particles about a mean trajectory is calculated using statistical methods. The particles concentration of about the mean trajectory is represented by a Gaussian probability density function, whose variance is based on the degree of particle dispersion due to turbulent fluctuations. Procedure predicts the turbulent dispersion of particles by integrating the trajectory equations for individual particles, using the instantaneous fluid velocity along the particle path during the integration.

The Discrete Random Walk (DRW) model is used. In this model, the fluctuating velocity components are discrete piecewise constant functions of time. Their random value is kept constant over an interval of time given by the characteristic lifetime of eddies. Prediction of the particle dispersion makes possible to use a concept of the integral time scale, T, which describes time spent in a turbulent motion along the particle path, dS:

$$T=\int_0^\infty\frac{u_p'(t)u_p'(t+s)}{\overline{u_p'^2}}ds.$$

In the DRW or "eddy lifetime" model a particle interaction with succession of the discrete stylized fluid phase turbulent eddies is simulated. Values of u', v', and w' that prevail during a lifetime of a turbulent eddy are sampled by assuming that they obey a Gaussian probability distribution, so that

$$u'=\xi\sqrt{\overline{u'^2}}$$

where ξ is a normally distributed random number.

The inert heating model is applied when a particle temperature is less than the vaporization temperature and after the volatile fraction of particle has been consumed. Procedure uses a simple heat balance to relate the particle temperature, $T_p(t)$, to the convective heat transfer and the absorption/emission of radiation at the particle surface:

$$m_p c_p \frac{dT_p}{dt} = hA_p(T_\infty - T_p) + \varepsilon_p A_p \sigma(\theta_R^4 - T_p^4)$$

where m_p is the mass of the particle; c_p is the heat capacity of the particle; A_p is the surface area of the particle; T_∞ is the local temperature of the continuous phase; h is the convective heat transfer coefficient; ε_p is the particle emissivity; σ is the Stefan-Boltzmann constant; θ_R is the radiation temperature.

The heat transfer coefficient, h, is evaluated using the correlation of Ranz and Marshall:

$$Nu = \frac{hd_p}{k_\infty} = 2.0 + 0.6\,\mathrm{Re}_d^{1/2}\,\mathrm{Pr}^{1/3},$$

where d_p is the particle diameter; k_∞ is the thermal conductivity of the continuous phase; Re_d is the Reynolds number based on the particle diameter and the relative velocity; Pr is the Prandtl number of the continuous phase.

The radiation temperature, $\theta_R = (G/4\sigma)^{1/4}$, where σ is the Stefan-Boltzmann constant, G is the incident radiation:

$$G = \int_{\Omega=4\pi} I d\Omega$$

where I is the radiation intensity, and Ω is the solid angle.

This equation is integrated in time using an approximate, linearized form that assumes that the particle temperature changes slowly from one time value to the next.

The devolatilization model is applied to a combusting particle when temperature of the particle reaches the vaporization temperature and remains in effect while the particle mass exceeds mass of the non-volatiles in the particle.

Heat transfer to the particle during the devolatilization process includes contributions from convection, radiation, and the heat value consumed during devolatilization:

$$m_p c_p \frac{dT_p}{dt} = hA_p(T_\infty - T_p) + \frac{dm_p}{dt} h_{fg} + \varepsilon_p A_p \sigma(\theta_R^4 - T_p^4).$$

After the volatile component of the particle is completely evolved, a surface reaction begins, which consumes a combustible fraction of the particle. The combusting particle may contain residual "ash" that reverts to the inert heating. Modeling the multiple particle surface reactions follows a pattern similar to the wall surface reaction models, where the surface species are now a "particle surface species". These species constitute the reactive char mass of the particle, hence, if the particle surface species are depleted, the reactive "char" content of the particle is consumed, and in turn, when the surface species are produced, they are added to the particle "char" mass.

The particle heat balance during a surface reaction is

$$m_p c_p \frac{dT_p}{dt} = hA_p(T_\infty - T_p) - f_h \frac{dm_p}{dt} H_{reac} + \varepsilon_p A_p \sigma(\theta_R^4 - T_p^4)$$

where H_{reac} is the heat released by the surface reaction.

The kinetic/diffusion-limited rate model assumes that the surface reaction rate is determined either by kinetics or by a diffusion rate. Procedure uses the model, in which a diffusion rate coefficient

$$D_0 = C_1 \frac{[(T_p + T_\infty)/2]^{0.75}}{d_p}$$

and a kinetic rate

$$R = C_2 e^{-(E/RT_p)}$$

are weighted to yield a char combustion rate of

$$\frac{dm_p}{dt} = -A_p p_{ox} \frac{D_0 R}{D_0 + R},$$

where A_p is the surface area of the droplet (πd_p^2), p_{ox} is the partial pressure of oxidant species in the gas surrounding the combusting particle, and the kinetic rate, R, incorporates the effects of chemical reaction on the internal surface of the char particle (intrinsic reaction) and pore diffusion.

It is taken into consideration six chemical reactions: particle surface (2-4) and volumetric (1, 5-6).

$$\mathrm{mv\_vol} + 1.706\ \mathrm{O_2} \rightarrow \mathrm{CO_2} + 1.543\ \mathrm{H_2O}, \quad (1)$$

$$\mathrm{C(s)} + 0.5\ \mathrm{O_2} \rightarrow \mathrm{CO}, \quad (2)$$

$$\mathrm{C(s)} + \mathrm{CO_2} \rightarrow 2\ \mathrm{CO}, \quad (3)$$

$$\mathrm{C(s)} + \mathrm{H_2O} \rightarrow \mathrm{H_2} + \mathrm{CO}, \quad (4)$$

$$\mathrm{H_2} + 0.5\ \mathrm{O_2} \rightarrow \mathrm{H_2O}, \quad (5)$$

$$\mathrm{CO} + 0.5\ \mathrm{O_2} \rightarrow \mathrm{CO_2}. \quad (6)$$

Particle size distribution after coal injection is defined by fitting the size distribution data to the Rosin-Rammler equation. In this approach, the complete range of particle sizes is divided into a set of discrete size ranges, each to be defined by a single stream that is part of the group.

The Rosin-Rammler distribution function is based on the assumption that an exponential relationship exists between the droplet diameter, d, and the mass fraction of droplets with diameter greater than d, Y_d:

$$Y_d = e^{-(d/\bar{d})^n}$$

where d is the mean diameter and n is the spread parameter.

C. Calculation Domain and Main Boundary Conditions

The reverse vortex plasma reformer is a simple 850 mm length and 180 mm ID three-dimensional duct depicted in Fig.

3. Inlet of the 3D duct is split out into two streams. The first high-speed air stream near the exit nozzle enters the duct through two rectangular feed apparatus with velocity magnitude 22 m/s and ten tangential channels of vortex generator with velocity magnitude 81 m/s corresponding a flow rate of 100 g/s. The coal stream enters the duct with velocities varying from 20 to 100 m/s and cone angle 70°. Both streams have temperature of 300 K. The coal particles enter reformer near the center of a duct with the mass flow rates of 5.85, 11.7, and 20.0 g/s. The duct wall is adiabatic. It was assumed that the region of intensive heat generation (due to inductive heating) is known from the experimental data. Partial combustion and coal gasification take place and products of these processes exit through the pressure-outlet. Presence of air feed apparatus, circular cavity and vortex generator leads to non-uniformity of pressure distribution in the air stream, and, hence, to three-dimensional effects which in a number of cases (especially at small air flow rates) result in radial flow precession [3].

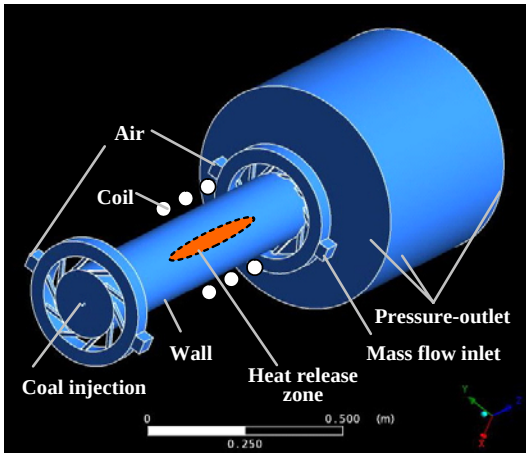

Fig. 3. Problem schematic.

The gasification products are considerably diluted with an air, which is injected from atmosphere, and, therefore, the flow structure inside the plasma reformer additionally depends on characteristics of the flow and mixing processes outside the exit nozzle. Therefore, a computational three-dimensional mesh was modified. In addition to the primary duct mesh the new computational region was added after the exit nozzle. The total number of tetrahedral cells is near 1 million.

The system of differential equations is completed by the following main boundary conditions (Fig. 3):

1) at the air inlet: $T = T_a$; $G = G_a$; $Y = Y_{O_2}$; $k = k_a$; $\varepsilon = \varepsilon_a$,

2) on the wall surfaces: no slip shear condition; $T = (q - q_r)/h_f + T_f$; zero diffusive flux; reflect boundary condition for the discrete phase,

3) on the pressure-outlet: gauge pressure = 0; backflow temperature = T_{sa}; $Y = Y_{O_2}$; $k = k_{sa}$; $\varepsilon = \varepsilon_{sa}$; escape boundary condition for the discrete phase,

4) at coal injection inlet: injection type – cone; diameter distribution – rosin-rammler; number of particle streams = 10; number of tries for discrete random walk model = 10

where $T_a, G_a, Y_{O_2}, k_a, \varepsilon_a$ are the air temperature, mass flow rate, mass fraction of oxygen, turbulence kinetic energy and turbulent dissipation rate accordingly; T_f is the local fluid temperature, q is the heat flux to the wall from a fluid cell; q_r is the radiative heat flux; h_f is the fluid-side local heat transfer coefficient; $T_{sa}, k_{sa}, \varepsilon_{sa}$ are the surrounding air temperature, turbulence kinetic energy and turbulent dissipation rate accordingly.

III. Results and Discussion

At the first stage using the ANSYS FLUENT computational program 3D calculations of heat exchange in a 1 MW plasma generator operating with direct and reverse vortexes are conducted at air flow rate of 100 g/s and without coal injection. Air was injected through ten tangential channels at the beginning or end of the cylindrical hybrid plasma torch chamber. It was assumed that the region of intensive heat release (due to inductive heating) in central part of the plasma generator is known from experimental data and radiant heat exchange is neglected. In calculations RNG *k*-ε-turbulence model, segregated solver, steady formulation, SIMPLE pressure-velocity coupling, and also approximations of thermal properties of air at high temperatures and atmospheric pressure were used.

Contours of mean axial velocity and temperature in cross-sections of the inductive type atmospheric pressure plasma torch with direct and reverse vortexes are shown in Fig. 4 and Fig. 5 accordingly. In direct vortex case recirculating zone in

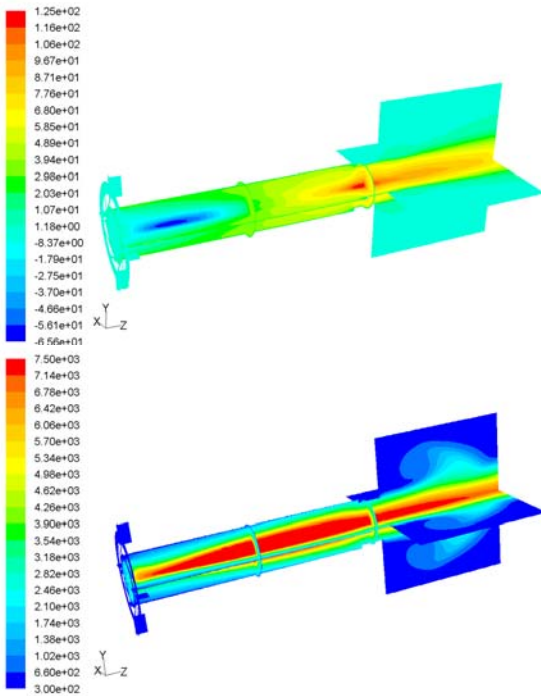

Fig. 4. Contours of mean axial velocity (m/s) and temperature (K) in a plasma torch with direct vortex.

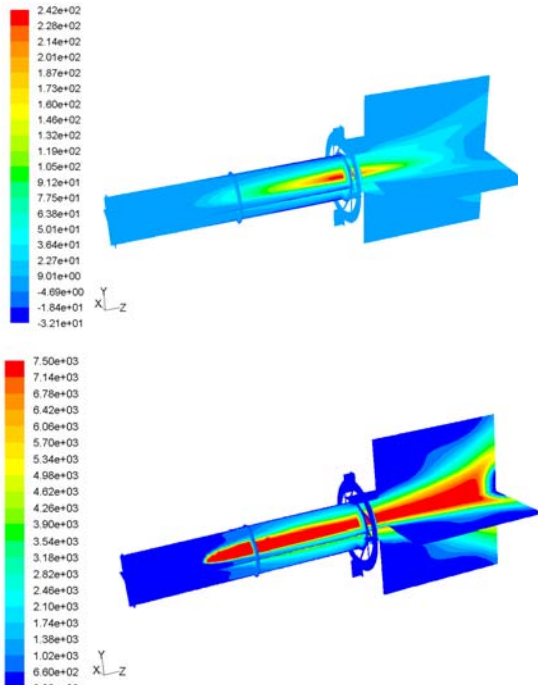

Fig. 5. Contours of mean axial velocity (m/s) and temperature (K) in a plasma torch with reverse vortex.

axial region of plasma chamber (negative values of axial velocities) takes place, resulting in heat transfer increasing in bottom part of the plasma generator. In reverse vortex case effective cooling of discharge chamber and bottom wall occurs, that considerably improve thermal conditions.

In case of 1 MW plasma power (corresponding to air flow rate of 100 g/s) for the reverse vortex mode and averaged by mass exit temperature 3569.4 K total wall heat transfer equals to 19.16 kW, including cylindrical, bottom part and exit walls heat transfer distribution as 78.15, 0.44, and 21.41 % accordingly. In case of direct vortex mode and averaged by mass exit temperature 3949.7 K total wall heat transfer equals to 85.97 kW with heat transfer distribution between cylindrical, bottom part and exit walls as 78.22, 2.93, 18.85 % accordingly. For these regime and designed parameters total wall heat transfer reduction due to reverse scheme application is about 65 kW that corresponds to the plasma generator efficiency increase on about 6.5 %. It is evident (Fig. 4, 5) that the temperature of bottom part of the plasma reformer is most essentially diminished. Calculated values of pressure losses are approximately equal for both cases.

At the second stage 3D calculations of coal gasification processes in a 1 MW reverse vortex plasma reformer are conducted. Air with temperature of 300 K is injected at the beginning or end of the cylindrical chamber for modeling direct and reverse vortex flow correspondingly. Air velocity magnitude is about 75 m/s in the exit section of the tangential channels.

Coal-mv particles with a cone angle 70° enter the plasma torch near the bottom center with a mass flow rate of 5.85, 11.7, and 20.0 g/s. Velocity magnitude of particles changes from 20 to 100 m/s. Particle size distribution is defined by fitting the size distribution data to the Rosin-Rammler equation. In this approach, the complete range of particle sizes is divided into a set of discrete size ranges, each to be defined by a single stream that is a part of the group. In a majority cases minimum diameter is 50 mkm; maximum diameter is 150 mkm; mean diameter is 110 mkm. Combustion (gasification) takes place and products exit plasma torch through the special nozzle. The multiple-surface reaction combustion model has been used.

The coal-mv vaporization temperature is 400 K; specific heat is 1000 J/(kg·K); density is 1300 kg/m^3; volatile component fraction is 28 %; combustible fraction is 64 %; binary diffusivity is $5\cdot10^{-4}$ m^2/s; swelling coefficient is 2.Temperature distribution inside the coal combustion system corresponds to a heat exchange in the discharge chamber. The coal-mv particles travel some distance before they start releasing volatiles. At this point, reaction starts and the temperature increases. This high temperature zone can be seen inside the plasma torch away from the inlet. In Finite Rate/Eddy Dissipation combustion, coal particles release volatiles that react with oxygen and produce combustion products. The stoichiometric coefficients can be calculated once chemical composition of coal volatiles is known. In direct vortex case coal particles (coal flow rate 20 g/s) have not enough residence time for complete particle surface reactions, including solid carbon (Fig. 6). Distribution of the DPM mass source in the plasma torch axial cross-section testifies this fact. For direct flow the "char" incomplete particle conversion degree constitutes 10.83 %, and for reverse flow 26.22 % for 5.85 g/s coal mass flow rate. In all cases the volatile content conversion is 100 %.

Dependences of static temperature, mass fraction of H_2, and

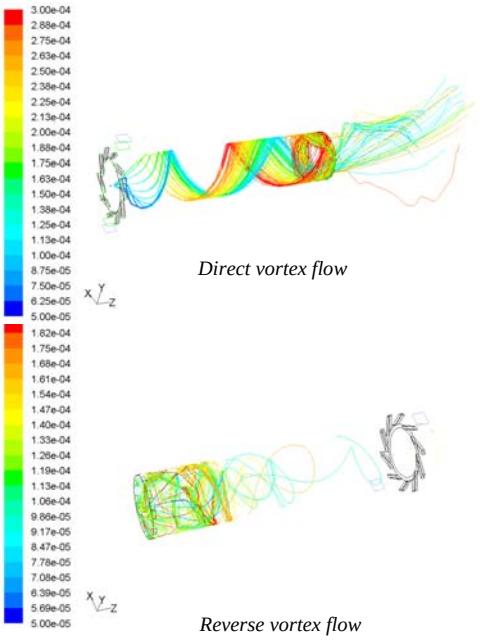

Fig. 6. Particle traces colored by particle diameter.

turbulence kinetic energy on the combustor length at the coal flow rate 11.7 g/s and different radius (axis of symmetry, 30 mm, and 60 mm) indicate different features of aerodynamic structure inside the inductive plasma torch with reverse flows and coal injection (Fig. 7).

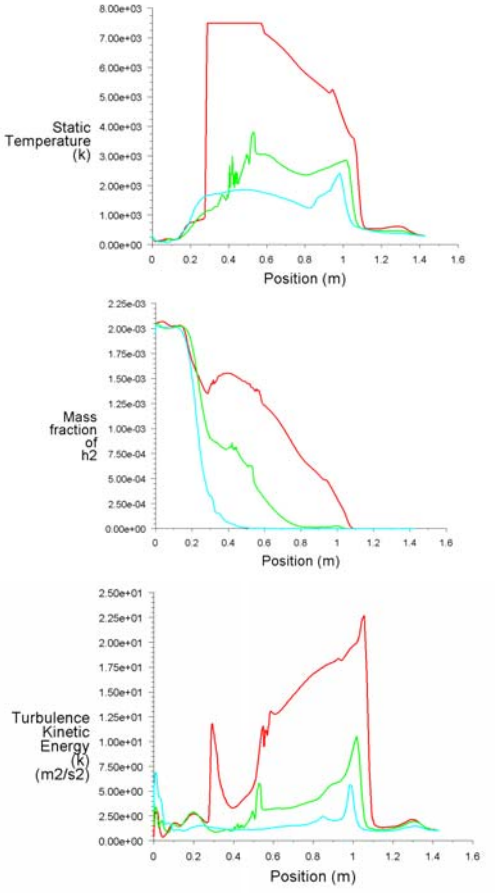

Fig. 7. Dependences of static temperature, mass fraction of H_2, and turbulence kinetic energy on the combustor length:
—— – r = 0 m; —— – r = 0.03 m; —— – r = 0.06 m.

The zone of maximum temperatures (near 7500 K) is in a central part of the plasma reformer (r = 0) and is determined by a coil location. As a result of the cold air reverse stream cooling effect the gas temperature is considerably diminished with walls approaching. Significant temperature variations in the cross-section r = 0.03 m is explained by different burnout velocity of coal particles in an atomization spectrum. Molecular hydrogen concentration values have maximum in a zone of primary mixing of gasified raw material with air, and further these concentrations are considerably decreased in accordance with a coal burnout. The level of turbulent energy has maximum in the paraxial sections at the region of the plasma reformer exit nozzle, where velocity gradients are very considerable.

The proposed hybrid plasma torch should combine advantages of the inductive type plasma torches with highly effective mean of the walls cooling and their thermal insulation as reverse vortex flow. It will also employ other type of relatively low plasma generator for additional media feeding, their initial activation and arc excitation. New hybrid plasma torch will operate as a multi-mode, multi-purpose, high power plasma system with wide range of plasma feedstock gases and turn down ratio, convenient and simultaneous feeding of several additional reagents into the discharge zone. It could be suitable for the waste processing systems, plasma chemical reactors, coating devices, mobile and autonomous small to mid-size coal gasification and hydrogen-rich gas generation systems, etc.

IV. Conclusion

Preliminary 3D-calculations of heat exchange in a 1 MW inductive type plasma reformer operating with direct and reverse vortexes are conducted at the air flow rate of 100 g/s. Proposed plasma torch should combine advantages of the inductive type plasma torches with highly effective mean of the walls cooling and their thermal insulation as reverse vortex flow can provide. For investigated regime and designed parameters reduction of the total wall heat transfer for the reverse scheme is about 65 kW that corresponds to the plasma generator efficiency increase by 6.5 %. The hybrid plasma torch could be suitable for waste processing systems, plasma chemical reactors, mobile and autonomous small to mid-size coal gasification and hydrogen-rich gas generation systems.

References

[1] I. Matveev, Applied Plasma Technologies, U.S. Patent Application for a "Triple Helical Flow Vortex Reactor", 11/309644, filed 02 Sept., 2006.

[2] I. Matveev, S. Serbin, "Experimental and Numerical Definition of the Reverse Vortex Combustor Parameters", *44th AIAA Aerospace Sciences Meeting and Exhibit*, Reno, Nevada, AIAA 2006-551, pp. 1-12, 2006.

[3] I. Matveev, S. Serbin, T. Butcher, N. Tutu, "Flow Structure investigation in a "Tornado" Combustor", *4th International Energy Conversion Engineering Conference and Exhibit (IECEC)*, San Diego, California, pp. 1-13, 2006.

[4] I. Matveev, S. Serbin, "Preliminary Design and CFD Modeling of a 1 MW Hybrid Plasma Torch for Waste Destruction and Coal Gasification", *2-nd Int. Workshop and Exhibition on Plasma Assisted Combustion (IWEPC)*, Falls Church, Virginia, pp. 43–44, 2006.

[5] Matveev, I., Matveeva, S., Gutsol, A., Fridman, A., "Non-Equilibrium Plasma Igniters and Pilots for Aerospace Application", *43d AIAA Aerospace Sciences Meeting and Exhibit*, Reno, Nevada, AIAA-2005-1991, 2005.

[6] Gutsol, A., Larjo, J., Hernberg, R., "Comparative calorimetric study of ICP generator with forward-vortex and reverse-vortex stabilization", *Plasma Chemistry and Plasma Processing*, Vol. 22 (3), pp. 351-369, 2002.

[7] Gutsol, A., Chirokov, A., Fridman, A., Worek, W. "Numerical Simulation of the Experimental ICP and Microwave plasma Torches with the Reverse Vortex Stabilization", *Proceedings of the 2nd International Conference on Computational Heat and Mass Transfer,* Rio de Janeiro, Brazil, 2001.

[8] Vlasov, V.I., "Theoretical investigations of high-temperature gas flow in HF-plasmatron discharge and working chambers", *Cosmonautics and Rocket Engineering*, № 23, pp. 18–26, 2001.

[9] Abele, D.V., Degres, G., "Numerical of High-Pressure Air Inductive Plasmas under Thermal and Chemical Non-equilibrium", *AIAA Paper*, 2000-2416, 2000.

[10] Bernardi, D., Colombo, V., Ghedini, E., Mentrelli, A., "Numerical simulation for the characterization of operating conditions of RF-RF hybrid plasma torches", *European Physical Journal D*, 28 (3), pp. 399-422, 2004.

[11] Bernardi, D., Colombo, V., Ghedini, E., Mentrelli, A., Trombetti, T., "3-D numerical simulation of fully-coupled particle heating in ICPTs", *European Physical Journal D*, 28 (3), pp. 423-433, 2004.

[12] Bernardi, D., Colombo, V., Ghedini, E., Mentrelli, A., "Three-dimensional modeling of inductively coupled plasma torches", *Pure and applied chemistry*, Vol. 77 (2), pp. 359-372, 2005.

[13] Amouroux, J., Dresvin, S., Morvan, D., et al., "Calculation of silicon particles dynamics, heat and mass transfers in thermal plasmas. Effect of particles vaporization", *High Temp. Mater. Proc.* 7 1, pp. 93-105, 2003.

[14] *The Electric Arc Column Theory. Low Temperature Plasma, Vol. 1*, Novosobirsk: Nauka, 1990.

[15] I. Matveev, S. Serbin, "Experimental and Numerical Definition of the Reverse Vortex Combustor Parameters", *44th AIAA Aerospace Sciences Meeting and Exhibit*, Reno, Nevada, AIAA 2006-551, pp. 1-12, 2006.

[16] B. E. Launder, D. B. Spalding, *Mathematical Models of Turbulence.* London: Academic Press, 1972.

[17] S. I. Serbin, "Modeling and Experimental Study of Operation Process in a Gas Turbine Combustor with a Plasma-Chemical Element", *Combust. Sci. and Tech.*, vol. 139, pp. 137–158, 1998.

[18] I. Matveev, S. Serbin, A. Mostipanenko, "Numerical Optimization of the ″Tornado″ Combustor Aerodynamic Parameters", *45th AIAA Aerospace Sciences Meeting and Exhibit*, Reno, Nevada, AIAA 2007-391, pp.1–12, 2007.

[19] V. I. Vlasov, "Numerical simulation of nonequilibrium flow in discharge chamber of RF-plasmatron", *Int. Conference "High-Speed Flow: Fundamental Problems"*, Zhukovsky, Russia, pp. 1–6, 2004.

[20] S. V. Dresvin, *The Fundamental of Theory and Design of H.F. Plasma Generators*, Leningrad: Energoatomizdat, 1991.

[21] G. N. Zalogin, B. A. Zemlyansky, V. B. Knotko et al., "High frequency plasmatron facility for investigation of aerophysical problems using high enthalpy gas flows", *Cosmonautics and Rocket Engineering*, № 2, pp. 22–32, 1994.

[22] D. Choudhury, *Introduction to the Renormalization Group Method and Turbulence Modeling*, Fluent Inc. Technical Memorandum TM-107, 1993.

Igor B. Matveev was born on February 11, 1954 in Russia. He received his Master of Science degree in mechanical engineering from the Nikolaev Shipbuilding Institute in 1977 and earned his Ph.D. degree in 1984. The Ph.D. theses were entitled "Development and Implementation of The Plasma Ignition Systems for Naval Gas Turbines".

From 1977 to 1990 was a researcher, teacher and associate professor of the Nikolaev Shipbuilding Institute. In 1990 established a privately owned company Plasmatechnika (Ukraine) for development and mass production of the plasma systems. From 2003 is with Applied Plasma Technologies (USA) as President & CEO.

Serhiy I. Serbin was born on April 29, 1958, in Mykolayiv, Ukraine. He received the M.S. (Dipl. Mech. Eng.) and Ph.D. (Cand. Sc. Tech.) degrees in mechanical engineering from the Mykolayiv Shipbuilding Institute, Ukraine, in 1981 and 1985, respectively, and the Dipl. D. Sc. Tech. and Dipl. Prof. degrees from the National University of Shipbuilding, Ukraine, in 1999 and 2002, respectively.

Since 1984, he has been working with the Ukrainian State Maritime Technical University as an Assistant Professor, Senior Lecturer, Associate Professor. Since 1999, he has been working with the National University of Shipbuilding as a Professor of Turbine Units Department. His research interests are plasma-chemical combustion, the techniques of intensifying the processes of hydrocarbon-fuels ignition and combustion in power engineering, combustion and plasma processes modeling.

Dr. Serbin is the Academician of Academy of Shipbuilding Sciences of Ukraine and International Academy of Maritime Sciences, Technologies and Innovations.